Petroleum and Coal

Article **Open Access**

Herschel-Bulkley Fluid Flow through an Annular Geometry with a Helically-Buckled Inner Pipe

Hicham Ferroudji[1], Ahmed Hadjadj[1], Zakarya Belimane[1], Mohamed Shafik Khaled[2] and Mohammad Azizur Rahman[3]*

[1] *Laboratory of Petroleum Equipment's Reliability and Materials, Faculty of Hydrocarbons and Chemistry, University of Boumerdes, Algeria*
[2] *Department of Petroleum Engineering, Texas A&M University, USA*
[3] *Department of Petroleum Engineering, Texas A&M University at Qatar, Qatar*

Received September 28, 2021; Accepted February 10, 2022

Abstract

A correct prediction of drilling fluid pressure drop is considered as a key parameter to carry out an efficient drilling operation and avoid non-productive time (NPT) during enrollment of the process. In this paper, a numerical approach is employed to analyze frictional pressure loss of Herschel-Bulkley (yield power-law) fluid flowing through an annular geometry in which the inner pipe makes a helical buckling motion in laminar and turbulent regimes. Results showed that rotation of the helically-buckled inner pipe induces a decrease of 10% and 6% of the pressure loss gradient of the Herschel-Bulkley fluid in the laminar regime for the helical pitch lengths of 6.9 m and 10 m, respectively. Also, increasing the pitch length of a helically-shaped inner pipe reduces the pressure loss gradient, particularly for low angular speeds. Moreover, the helical pitch length increment from 6.9 m to 10.7 m slightly affects the pressure loss gradient for the turbulent regime.

***Keywords**: CFD approach; Helical buckling; Frictional pressure loss; Herschel Bulkley fluid; Laminar and turbulent flow regime.*

1. Introduction

Accuracy of frictional pressure drop estimation is the most crucial parameter in the hydraulics program of drilling, which depends on geometrical characteristics (eccentricity, diameters ratio, annulus shape, etc.) and fluid properties (density, rheology, and flow regime). Numerous experimental and numerical investigations have been done about the flow of non-Newtonian fluids in the annulus where the inner pipe makes only pure rotation [1-6]. However, in the real case, complicated motions of the inner pipe may occur during drilling operations, including helical buckling motion [7]. In the literature, there is still a lack of the effect of buckling motion on the hydrodynamics of drilling fluids.

To consider the real motions of a drill pipe during a drilling process, Saasen [8] mentioned that drill string motion has a significant effect on frictional pressure loss and should be taken into consideration. Mitchell [9] studied drill string transition from straight pipe to lateral buckling (snake buckling) and from lateral buckling to helical buckling for different deviations of a wellbore, as can be seen in Figure 1.

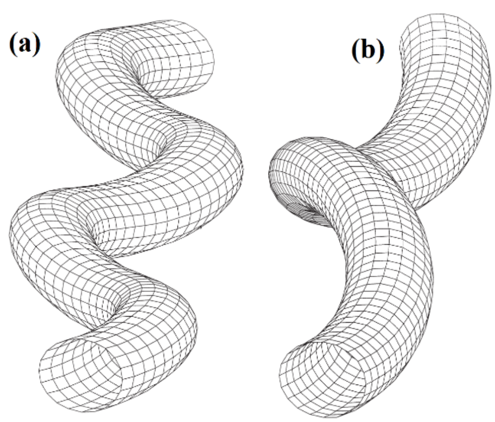

Figure 1. (a) Lateral buckling (snake buckling), (b) helical buckling [13]

Based on theoretical models, He *et al.* [10] found that the applied torque affects the buckling shape of a drill string by reducing the critical buckling compressional force (weight on the bit). Moreover, Chen *et al.* [11] concluded that the necessary force for helical buckling is 1.4 times greater than the required force for sinusoidal buckling.

Erge *et al.* [12] conducted an experimental study of Herschel-Bulkley fluid flow through an annular space where the inner cylinder has a helical shape with different pitch lengths. They observed that the helical shape of the inner cylinder could significantly reduce frictional pressure loss. In addition, they found that rotation of the helically-buckled pipe results in a significant increase in frictional pressure loss as compared to the case of a straight inner pipe.

Buckling will not necessarily occur at the same time in all parts of the drill pipe. In long drill pipes, the axial force (weight on the bit WOB) acting on each point of the string is different, resulting in a partially buckled drill pipe. Therefore, other sections of the buckled drill pipe will be at various stages of the buckling process. In addition, even the helically shaped part of the drill pipe may have different pitch lengths [13]. The same observations were made by Huang *et al.* [14], as can be seen in Figure 2.

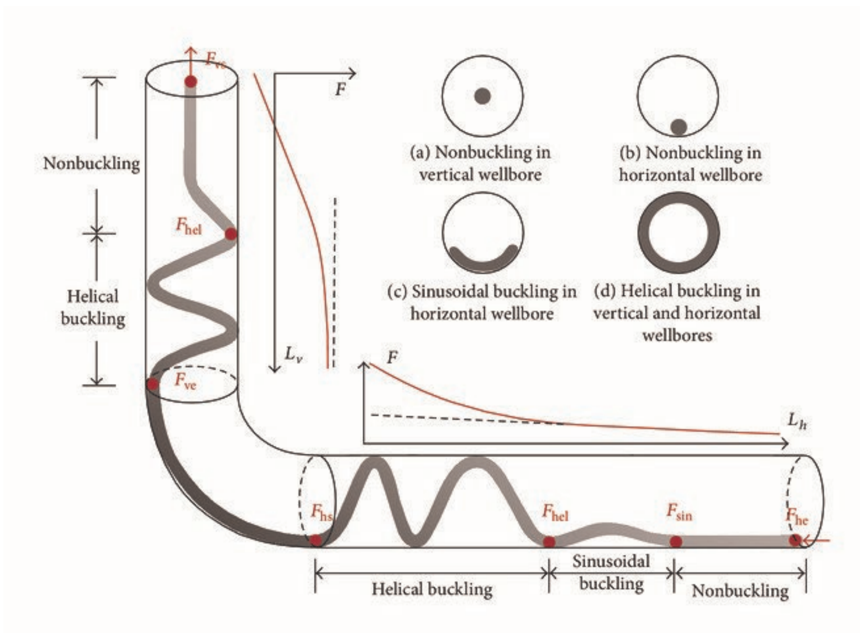

Figure 2. Different types of drill pipe buckling in a horizontal well [14]

There are few attempts to evaluate the effect of various drill pipe motions on the flow of drilling fluids through annular geometries [15-20]. However, there is still a need to understand more about the behavior of drilling fluids when the helical motion of a drill pipe takes place. In this paper, the influence of fluid velocity and rotation of the helically-Buckled inner pipe on frictional pressure loss of yield power-law in laminar and turbulent regime flowing through an annular geometry for different helical pitch lengths are discussed based on CFD approach using ANSYS-Fluent 19.5.

2. Materials and methods

2.1. Physical model

The eccentricity will not be constant through a wellbore, especially in deviated and horizontal sections. In a real wellbore, a part of the drill pipe will experience compression due to the rotation and the applied weight. As a result, a variable eccentricity will be present (sinusoidal buckling). At high compression, the drill string deforms, resulting in helical buckling patterns, as shown in Figure 3.

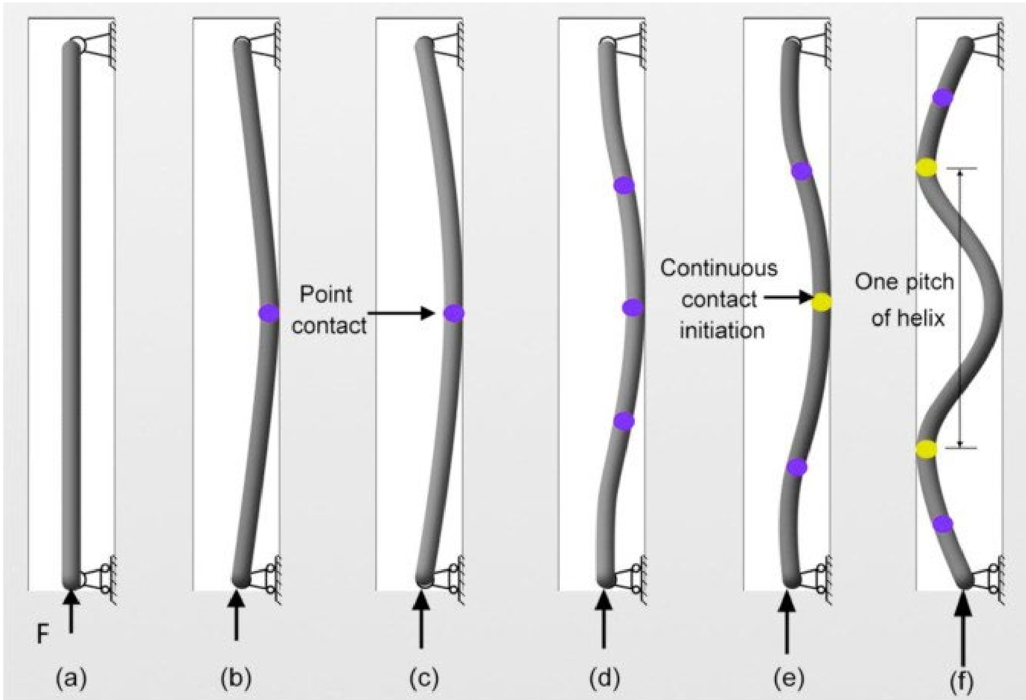

Figure 3. Helical buckling stages of a drill pipe [23]

In this work, the helical deformation of the buckling process is considered since the sinusoidal deformation is generally transient. In this case, the effects of the angular speed of the helically-buckled inner pipe on frictional pressure loss of a Herschel-Bulkley fluid in both laminar and turbulent regimes for various fluid velocities, helical pitch lengths, yield stresses, and flow behavior indexes are analyzed.

2.2. Mathematical equations

The flow of the Herschel-Bulkley fluid (yield power-law) through an annular geometry with a helically-buckled inner pipe is assumed to be fully developed, steady, incompressible, and isothermal in laminar and turbulent regimes.

The continuity and momentum equations that govern the flow can be listed as follows:

$$\frac{\partial v_x}{\partial x}+\frac{\partial v_y}{\partial y}+\frac{\partial v_z}{\partial z}=0 \tag{1}$$

$$\rho\left(\frac{\partial v_x}{\partial t}+v_x\frac{\partial v_x}{\partial x}+v_y\frac{\partial v_x}{\partial y}+v_z\frac{\partial v_x}{\partial z}\right)=-\frac{\partial P}{\partial x}-\left[\frac{\partial \tau_{xx}}{\partial x}+\frac{\partial \tau_{yx}}{\partial y}+\frac{\partial \tau_{zx}}{\partial z}\right]+\rho g_x \tag{2}$$

$$\rho\left(\frac{\partial v_y}{\partial t}+v_x\frac{\partial v_y}{\partial x}+v_y\frac{\partial v_y}{\partial y}+v_z\frac{\partial v_y}{\partial z}\right)=-\frac{\partial P}{\partial y}-\left[\frac{\partial \tau_{xy}}{\partial x}+\frac{\partial \tau_{yy}}{\partial y}+\frac{\partial \tau_{zy}}{\partial z}\right]+\rho g_y \tag{3}$$

$$\rho\left(\frac{\partial v_z}{\partial t}+v_x\frac{\partial v_z}{\partial x}+v_y\frac{\partial v_z}{\partial y}+v_z\frac{\partial v_z}{\partial z}\right)=-\frac{\partial P}{\partial z}-\left[\frac{\partial \tau_{xz}}{\partial x}+\frac{\partial \tau_{yz}}{\partial y}+\frac{\partial \tau_{zz}}{\partial z}\right]+\rho g_z \tag{4}$$

where v_x, v_y and v_z are the velocity components; P is the pressure; ρ is the density; g is the gravity.

Furthermore, the shear rate magnitude is calculated based on the following expression [21]:

$$|\dot{\gamma}|=2\left[\left(\frac{\partial v_x}{\partial x}\right)^2+\left(\frac{\partial v_y}{\partial y}\right)^2\left(\frac{\partial v_z}{\partial z}\right)^2\right]+\left(\frac{\partial v_x}{\partial y}+\frac{\partial v_y}{\partial x}\right)^2+\left(\frac{\partial v_x}{\partial z}+\frac{\partial v_z}{\partial x}\right)^2+\left(\frac{\partial v_y}{\partial z}+\frac{\partial v_z}{\partial y}\right)^2 \tag{5}$$

Assuming a fully developed turbulent flow, a realizable k-ε model is used, which is a turbulent viscosity based two-equation turbulence model [21]. The model is especially suitable for the present case since it was observed to deliver comparably accurate results for secondary flow and strong streamline curvature [22].

The rheological behavior if a Herschel-Bulkley fluid is expressed as follows:

$$\tau=\tau_0+K(\dot{\gamma})^n \tag{6}$$

where τ_0 is the yield stress; K represents the flow consistency index; and n stands for the flow behavior index.

The rheological parameters of the adopted fluid are shown in Table 1 as follows:

Table 1. Fluid and geometry characteristics

Rheological behavior	Fluid and geometry characteristics				
	K [Pa.sn]	n [-]	Do [mm]	τ_0 [Pa.sn]	Di [mm]
Non-Newtonian	2.44	0.33	50.8	4.09	25.4

The helical shape of the inner pipe is modeled by considering the parametric equations of the centerline of the inner cylinder (Helix). The parametric equations of a helix are expressed as follows:

$$x(t) = r \times cos(t) \quad (7)$$

$$y(t) = r \times sin(t) \quad (8)$$

$$z(t) = c \times t \quad (9)$$

where r is the radius of the helix and $2 \times \pi \times c$ is a constant giving the helical pitch length of the helically-buckled inner pipe.

In the real case, when a helical buckling occurs, the drill pipe is in contact with the casing. For that, to perform simulations, the annular geometry is considered almost fully eccentric ($E = 0.95$) along the inner pipe to assure the stability of numerical calculation process, as well as, to maintain the quality of the mesh. On the other side, the eccentricity of the outer and inner cylinders is determined according to the following relationship:

$$E = \frac{2.e}{(D_o - D_i)} \quad (10)$$

where e is the offset distance from the concentric position.

2.3. Simulation method

The number of the considered hexahedral elements to carry out the numerical simulations is determined through mesh sensitivity analysis, where this number needs to be at least 750000 elements to ensure the accuracy of results, as shown in Figure 4. This mesh sensitivity analysis is performed using a Herschel-Bulkley fluid flow in laminar regime with a helical shape of the inner pipe (pitch length of 6.9 m). In addition, the data for the sensitivity analysis is taken from the experimental study by Erge *et al.* [12]. In the present work, a mesh of 800000 elements (20 radial portions, 80 circumferential portions, and 500 axial portions) is adopted to ensure that the results are mesh-independent, as well as, maintaining the number of elements as low as possible to optimize computational time. A 3D view of the utilized mesh is illustrated in Figure 5.

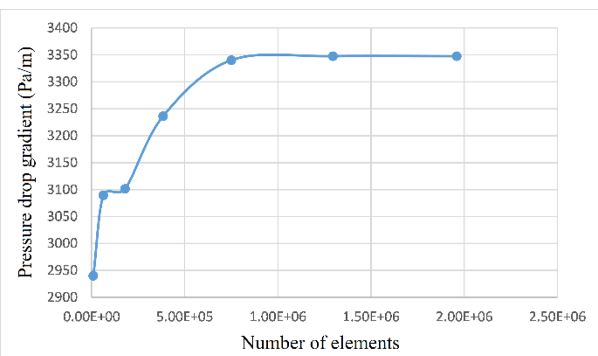

Figure 4. Mesh sensitivity ($U = 1$ m/s, pitch = 6.9 m)

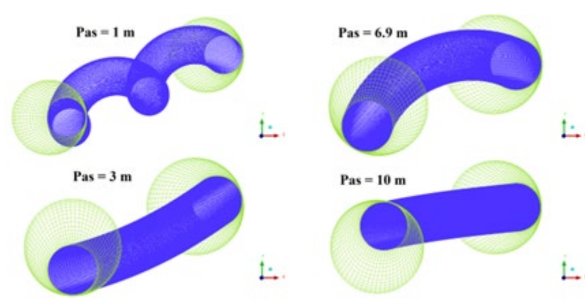

Figure 5. 3D view of the considered mesh

Since the inner pipe has a helical shape and rotates around the center of the outer pipe, the moving mesh approach is utilized to model this motion. For that, the annular geometry is split into two regions: i) static region, which is near the wall of the outer pipe and not influenced by the motion of the inner pipe, ii) moving region, which is influenced by the motion of the inner pipe. In addition, the two regions are related with an interface to transfer velocity, pressure, and other outputs, as shown in Figure 6. Therefore, rotation of the inner region around the center of the outer pipe represents the angular speed of the drill pipe in the real case.

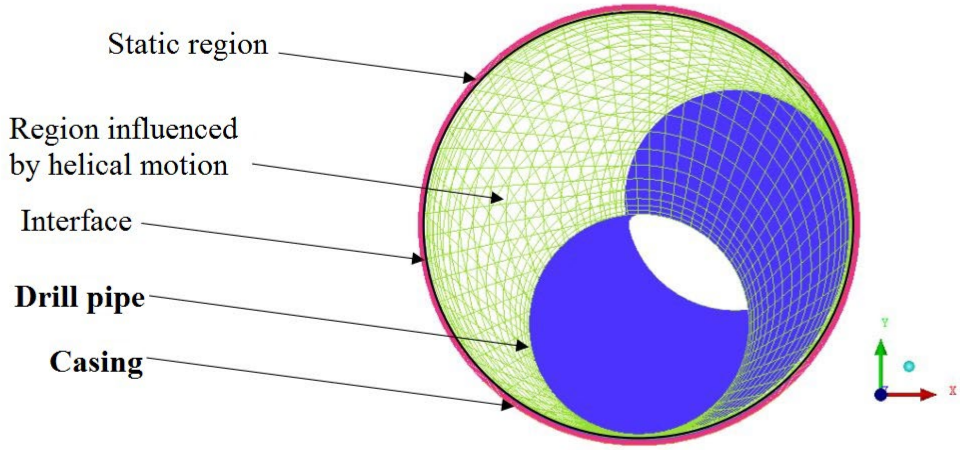

Figure 6. Mesh cross-section (pitch = 6.9 m)

The numerical approach of Finite Volume Method (FVM), which is the basis for the commercial code ANSYS Fluent 19.5 is employed to solve the differential equations describing the physical phenomena, where the flow equations are integrated over each control volume. Besides, since the moving mesh is considered, transient modeling is needed where the position of the inner pipe is updated according to the angular speed each time step. PRESTO scheme and SIMPLE algorithm are used for discretization of pressure and coupling pressure-velocity, respectively. While, first-order upwind is employed to discretize the momentum equation instead of higher-order levels to maintain the stability of the iterative calculation process and avoid perturbations, particularly in the presence of moving mesh. Also, a time step of 10^{-4} allowed to attaining a convergence of at least 10^{-5}.

2.4. Validation model

The collected numerical results of the Herschel-Bulkley flow through an annular space with a helical shape of the inner cylinder are compared with experimental data from work done by Erge *et al.* [12], as shown in Figure 7.

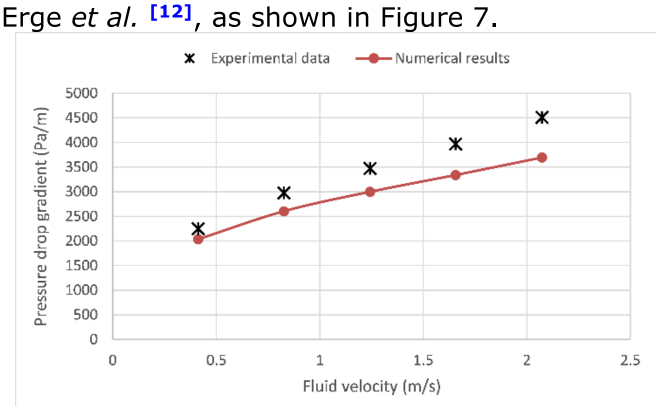

Figure 7. Comparison of the numerical results with experimental data of Erge *et al.* [12] (120 rpm)

A good matching between the numerical and experimental results is observed, where the mean error is estimated to be around 9%. It is worth mentioning that the discrepancy between the experimental and numerical results for high fluid velocities can be attributed to the formation of small turbulence eddies initiating the turbulent regime to occur. This comparison shows that the CFD method coupled with the moving mesh approach can handle such kind of drill pipe motion and provide accurate predictions.

3. Results and discussion

3.1. Laminar regime

Effects of angular speed of the inner pipe on pressure loss gradient of Herschel-Bulkley flowing in laminar for various helical pitch lengths are shown in Figure 8. As can be seen, a slight increase in pressure loss gradient is caused when the angular speed increases from 0 rpm to 50 rpm due to the inertial effects induced by the inner cylinder motion. Then the pressure loss gradient begins to diminish when the angular speed is within the range of 50 rpm to 150 rpm. This decrease is probably induced by the shear-thinning phenomenon of the Hershel-bulkley fluid. For the range of 150 rpm to 400 rpm, the pressure loss gradient decreases gradually. Therefore, the overall decrease in the pressure loss gradient is estimated to be 10% and 6% for the helical pitch lengths of 6.9 m and 10 m, respectively.

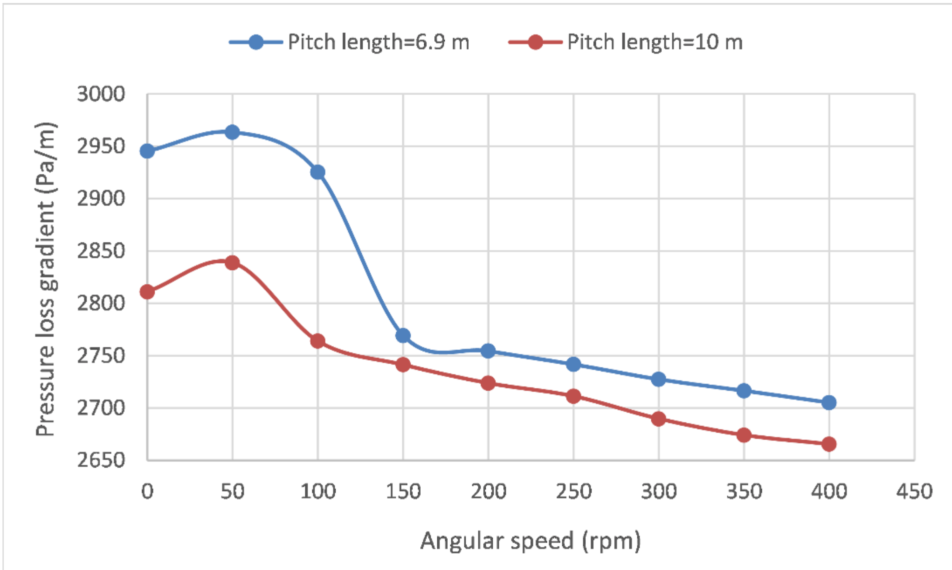

Figure 8. Influence of the angular speed of helically-shaped inner pipe on pressure loss gradient of Herschel-Bulkley fluid in laminar regime for various helical pitch lengths ($U = 1$ m/s, $\tau_0 = 4.09$ Pa, $n = 0.33$)

An opposite effect is found from the work of Erge *et al.* [12] where they indicated that increment of the angular speed of helically-shaped pipe results in a slight rise of pressure loss gradient. This disagreement can be explained by the imperfect helical shape of the inner pipe of the considered experimental setup, as well as by the totally eccentric annular unlike the present numerical work where the eccentricity is considered to be at ($E = 0.95$) to avoid the difficulties of numerical calculations. On the other hand, increasing the pitch length of a helically-shaped inner pipe (decreasing the extent of the helical shape) leads to a reduction in the pressure loss gradient, in particular for low angular speeds. This behavior is also observed by Asafa and Shah [24] for a static inner pipe and the change in flow direction can explain it due to the decrease in the flow path length as the helical pitch length of the helical inner pipe increases.

Figure 9 shows how the Herschel-Bulkley fluid pressure loss gradient behaves as the angular speed of the helically-shaped inner pipe increases from 0 rpm to 400 rpm for different flow velocities. As shown, increasing the angular speed from 0 rpm to 400 rpm reduces the pressure loss gradient by approximately 20%, 9%, and 6% for the fluid velocities of 0.5 m/s, 1 m/s, and 1.5 m/s, respectively. However, rotation of the helically-shaped inner pipe is found to cause a marginal effect on pressure loss gradient for the fluid velocity of 2 m/s. Thus, the angular speed has a slight impact on pressure loss gradient as the flow regime approaches the transition phase before the turbulent regime occurs in the annular space.

The effect of angular speed of the inner pipe on the evolution of the Herschel-Bulkley pressure loss gradient for various yield stresses is depicted in Figure 10. This figure shows that rotation of the helically-shaped inner pipe diminishes the pressure loss gradient of the Herschel-Bulkley fluid, where this reduction is estimated at 16%, 13%, and 8% for the yield stresses of 12 Pa, 8 Pa, and 4.09 Pa, respectively. However, for the yield stress of $\tau_0 = 0$ Pa, the angular speed has a marginal effect. This behavior can be credited to the shear-thinning phenomena, where the latter can be enhanced with the increase of the yield stress of the Herschel-Bulkley fluid. For instance, increasing the weight concentration of the Xanthan Gum

(XG) increases the yield stress. It improves the shear-thinning behavior (reduction in the flow behavior index) of the Herschel-Bulkley fluids, particularly for high shear rates [25-26]. This can explain the decrease in the pressure loss gradient, in particular for high yield stress values.

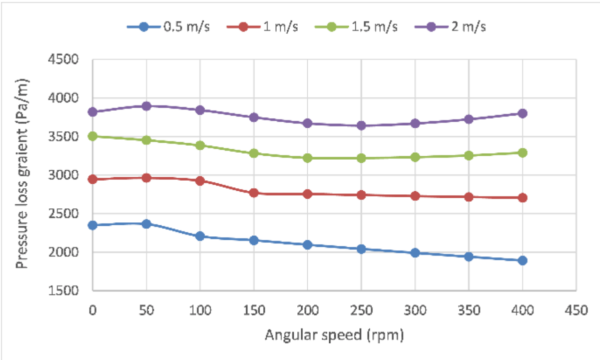

Figure 9. Influence of the angular speed of helically-shaped inner pipe on pressure loss gradient of Herschel-Bulkley fluid in laminar regime for various fluid velocities (pitch length = 6.9 m, τ_0 = 4.09 Pa, n = 0.33)

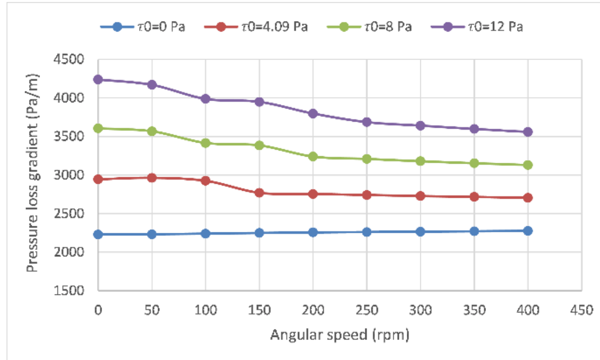

Figure 10. Influence of the angular speed of helically-shaped inner pipe on pressure loss gradient of Herschel-Bulkley fluid in laminar regime for various yield stress values ($U = 1$ m/s, pitch length = 6.9 m, n = 0.33)

3.2. Turbulent regime

Figure 11 describes the behavior of the pressure loss gradient under turbulent conditions for different pitch lengths of the helical inner cylinder as the angular speed increases from 0 rpm to 400 rpm. As shown, increasing the rotation of the inner pipe induces a slight increase in the pressure loss gradient for all pitch lengths. The marginal effect of the angular speed of the inner pipe indicates that the flow is dominated by turbulence, where the motion of the inner pipe intensifies the vortices of the turbulent regime in the annulus.

Figure 12 shows how the Herschel-Bulkley fluid pressure loss gradient behaves as the fluid velocity increases from 4 m/s to 5.5 m/s for different helical pitch lengths. As shown, the pressure loss gradient rises linearly with the fluid velocity, where the pitch length of the helical shape of the inner cylinder has a slight effect. Therefore, it can be concluded that the considered pitch lengths (from 6.9 m to 10.7 m) have a marginal impact on pressure loss gradient when the Herschel-Bulkley fluid flows in a turbulent regime.

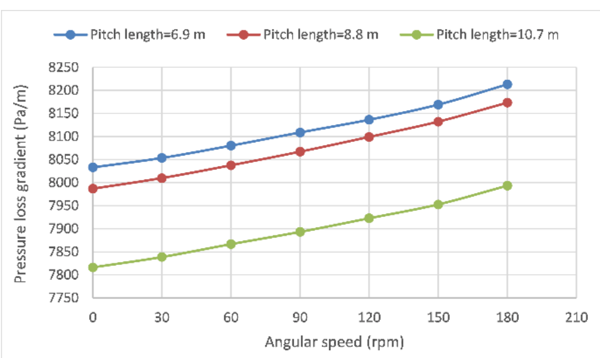

Figure 11. Influence of the angular speed of helically-shaped inner pipe on pressure loss gradient of Herschel-Bulkley fluid in turbulent regime for various helical pitch lengths ($U = 4$ m/s, $\tau_0 = 4.09$ Pa, n = 0.33)

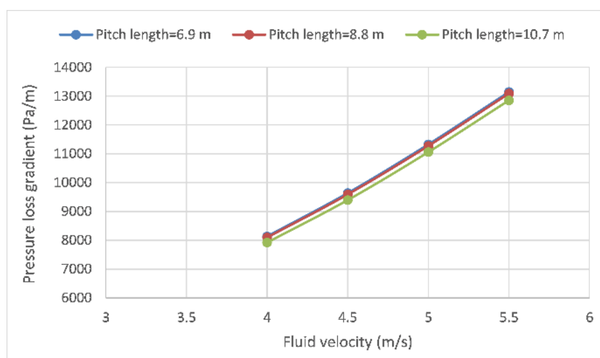

Figure 12. Influence of the fluid velocity on pressure loss gradient of Herschel-Bulkley fluid in turbulent regime for various helical pitch lengths ($\tau_0 = 4.09$ Pa, n = 0.33, 120 rpm)

4. Conclusions

In this investigation, the moving mesh technique is considered to simulate the flow of a Herschel-Bulkley in a laminar and turbulent regime through an annular geometry in which the inner pipe has a helical shape. The following can be concluded from this work:

- Due to the domination of the shear-shinning effect, rotation of the helically-buckled inner pipe induces a decrease of 10% and 6% of the pressure loss gradient of the Herschel-Bulkley fluid in the laminar regime for the helical pitch lengths of 6.9 m and 10 m, respectively.
- Increasing the pitch length of a helically-shaped inner pipe reduces the pressure loss gradient, particularly for low angular speeds.
- Both angular speed and helical pitch length from 6.9 m to 10.7 m have a slight effect on the pressure loss gradient for the turbulent regime

Acknowledgment

This publication was made possible by the grant NPRP10-0101-170091 from Qatar National Research Fund (a member of the Qatar Foundation). Statements made herein are solely the responsibility of the authors. Authors also very thankful to Minsoo Jang for helping to collect data and analysis.

Nomenclature

D_0	*diameter of the outer cylinder (m)*
D_i	*diameter of the inner cylinder (m)*
r	*radius of helix centreline*
E	*eccentricity of the inner cylinder (-)*
τ_0	*yield stress (Pa)*
K	*flow consistency index (Pa.s^n)*
n	*flow behavior index (-)*
u	*bulk flow velocity (m/s)*
ρ	*fluid density (kg/m^3)*
$\dot{\gamma}$	*shear rate (s^{-1})*

References

[1] Ahmed RM, Miska SZ. Experimental study and modeling of yield power-law fluid flow in annuli with drillpipe rotation. In IADC/SPE Drilling Conference. OnePetro 2008.

[2] Ferroudji H, Hadjadj A, Haddad A, & Ofei TN. Numerical study of parameters affecting pressure drop of power-law fluid in horizontal annulus for laminar and turbulent flows. Journal of Petroleum Exploration and Production Technology, 2019; 9(4), 3091-3101.

[3] Rasul G, Qureshi,MF, Ferroudji H, Butt S, Hasan R, Hassan I, Rahman MA. Analysis of cuttings transport and flow pattern in nearly horizontal extended reach well. Journal of Advanced Research in Fluid Mechanics and Thermal Sciences, 2020; 71(2), 69-86.

[4] Ferroudji H, Hadjadj A, Rahman MA, Hassan I, Maheshwari P, Odan MA. Study of Ostwald-de Waele fluid flow in an elliptical annulus using the slot model and the CFD approach. Journal of Dispersion Science and Technology, 2021; 42(9), 1395-1407.

[5] Qureshi MF, Ali MH, Ferroudji H, Rasul G, Khan MS, Rahman MA, Hassan I. Measuring solid cuttings transport in Newtonian fluid across horizontal annulus using electrical resistance tomography (ERT). Flow Measurement and Instrumentation, 2021; 77, 101841.

[6] Belimane Z, Hadjadj A, Ferroudji H, Rahman MA, & Qureshi MF. Modeling surge pressures during tripping operations in eccentric annuli. Journal of Natural Gas Science and Engineering, 2021; 104233.

[7] Erge O, Ozbayoglu ME, Miska SZ, Yu M, Takach N, Saasen A, May R. Effect of drillstring deflection and rotary speed on annular frictional pressure losses. Journal of Energy Resources Technology, 2014; 136(4).

[8] Saasen A. Annular frictional pressure losses during drilling—predicting the effect of drillstring rotation. Journal of Energy Resources Technology, 2014; 136(3).

[9] Mitchell RF. Effects of well deviation on helical buckling. SPE Drilling & Completion, 1997; 12(01), 63-70.

[10] He X, Halsey GW, Kyllingstad A. Interactions between torque and helical buckling in drilling. In SPE annual technical conference and exhibition. OnePetro 1995.

[11] Chen VC, Lin VH, & Cheatham JB. An analysis of tubing and casing buckling in horizontal wells. In Offshore Technology Conference. OnePetro 1989.

[12] Erge O, Ozbayoglu ME, Miska SZ, Yu M, Takach N, Saasen A, May R. Effect of drillstring deflection and rotary speed on annular frictional pressure losses. Journal of Energy Resources Technology, 2014; 136(4).

[13] Cunha JC. Buckling of tubulars inside wellbores: a review on recent theoretical and experimental works. In SPE Production and Operations Symposium. OnePetro 2003.

[14] Huang W, Gao D, Liu Y. Prediction model of mechanical extending limits in horizontal drilling and design methods of tubular strings to improve limits. Mathematical Problems in Engineering, 2017.

[15] Demiralp Y. Effects Of Drill-pipe Whirling Motion on Cuttings Transport Performance for Horizontal Drilling, 2014.

[16] Bicalho IC, Dos Santos DBL, Ataíde CH, Duarte CR. Fluid-dynamic behavior of flow in partially obstructed concentric and eccentric annuli with orbital motion. Journal of Petroleum Science and Engineering, 2016; 137, 202-213.

[17] Ferroudji H, Hadjadj A, Ofei TN, Rahman M A, Hassan I, Haddad A. CFD method for analysis of the effect of drill pipe orbital motion speed and eccentricity on the velocity profiles and pressure drop of drilling fluid in laminar regime. Petroleum and Coal, 2019; 61(5), 1241-1251.

[18] Ferroudji H, Hadjadj A, Ofei TN, Rahman MA. The effect of orbital motion and eccentricity of drill pipe on pressure gradient in eccentric annulus flow with Newtonian and non-Newtonian fluids. Progress in Computational Fluid Dynamics, an International Journal, 2020; 20(4), 238-247.

[19] Pang B, Wang S, Jiang X, Lu H. Effect of orbital motion of drill pipe on the transport of non-Newtonian fluid-cuttings mixture in horizontal drilling annulus. Journal of Petroleum Science and Engineering, 2019; 174, 201-215.

[20] Busch A, Johansen ST. Cuttings transport: On the effect of drill pipe rotation and lateral motion on the cuttings bed. Journal of Petroleum Science and Engineering, 2020; 191, 107136.

[21] Fluent A. 12.0 Theory Guide, Vol. 5, Ansys Inc 2009, USA

[22] Shih TH, Liou WW, Shabbir A, Yang Z, Zh, J. A new k-ϵ eddy viscosity model for high reynolds number turbulent flows. Computers & fluids, 1995; 24(3), 227-238.

[23] Huang W, Gao D, Liu Y. A study of tubular string buckling in vertical wells. International Journal of Mechanical Sciences, 2016; 118, 231-253.

[24] Asafa KA, Shah SN. Effect of coiled tubing buckling on horizontal annular flow. In SPE/ICoTA Coiled Tubing & Well Intervention Conference and Exhibition. OnePetro 2012.

[25] Moukhametov R, Srivastava A, Akhter S, Bautista J, Ferroudji H, Hadear H, Rahman MA. Effects of salinity on solid particle settling velocity in non-Newtonian Herschel–Bulkley fluids. Journal of Petroleum Exploration and Production Technology, 2021; 1-15.

[26] Rushd S, Hassan I, Sultan RA, Kelessidis VC, Rahman A, Hasan HS, Hasan A. Terminal settling velocity of a single sphere in drilling fluid. Particulate Science and Technology, 2019; 37(8): 943-952.

To whom correspondence should be addressed: Dr. Hicham Ferroudji, Laboratory of Petroleum Equipment's Reliability and Materials, Faculty of Hydrocarbons and Chemistry, University of Boumerdes, Algeria,
E-mail: hichamf32@gmail.com, ferroudji.h@univ-boumerdes.dz